



An innovative formulation for buckling analysis of nano-tapered Timoshenko beams with axially varying materials

Elahe Aghaei ^a, Masoumeh Soltani ^a, Azadeh Soltani ^a, Rossana Dimitri ^b, Francesco Tornabene ^b

^a Department of Civil Engineering, Faculty of Engineering, University of Kashan, Kashan, Iran

^b Department of Innovation Engineering, Faculty of Engineering, Università del Salento, Lecce, Italy

Abstract

This paper presents a novel and low-cost formula based on the first-order shear deformation theory and Eringen's nonlocal elasticity theory for the stability analysis of tapered Timoshenko nanobeams with axially varying materials. The coupled governing differential equations of the problem, involving both the transverse displacements and rotations, stem from the energy method. Based on a mathematical manipulation, the system of equilibrium equations is converted to a novel single fifth-order differential equation with variable coefficients in terms of the vertical deflection, which is solved numerically to obtain the axial buckling load. The accuracy of the proposed formulation is first verified against the available literature, with the additional advantage related to its reduced computational effort, compared to other formulations. A systematic investigation is, thus, performed to check for the influence of the non-local parameter, power-law index, tapering ratio and length-to-thickness aspect ratio on the linear buckling strength of simply supported functionally graded nano-tapered Timoshenko beams. Due to the generality of the derived formula, it can be adjusted for the optimal design of Timoshenko nanobeams with favorable axial changes in material properties as well as the geometrical features.

Keywords: Axially functionally graded materials; Differential quadrature method; Nonlocal elasticity theory; Stability analysis; Variable cross-section.

1. Introduction

In recent years, the expansion of nanoscience and nanotechnology has received considerable interest. The micro/nano-scaled structural elements such as beams, shells, and plates are extensively adopted as key components in different modern engineering devices, including sensors, actuators, transistors, probes, and nano-electromechanical systems (NEMS). It is important to note that properties of materials, such as electrical conductivity, thermal performance, stiffness, and strength, can change by decreasing the size scale. Such an important aspect is well known as the size effect. Since this property cannot be taken into account through classical elastic theories, due to the neglecting the material length scale parameter in their mathematical formulation, various higher order continuum theories have been proposed in the literature to account for any small-size effect, such as the modified couple stress theory, the strain gradient elasticity theory [1], the surface energy theory [2], and the nonlocal elasticity theory [3, 4]. Among them, the nonlocal elasticity theory [3] proposed by Eringen is widely employed by many researchers due to

its practicality and computational simplicity. This theory assumes that the stress state at an arbitrary point in an elastic body is considered as a function of strains of all other points in that continuum.

With the development of high technology and fabrication processes, the practical application of micro- and nanoscale structural components made of functionally graded materials (FGMs) in most innovative and sensitive engineering systems and devices, such as atomic force microscopes, sensors, oscillators, nano/micro electro-mechanical systems (NEMS/MEMS) and actuators, has become very common in the last decades. Due to their desirable characteristics, indeed, FGMs are capable to eliminate or minimize the interfacial stress concentrations, as well as the multifunctionality thermal resistance and optimal distribution of weight. In such a context, various studies have been conducted in literature to investigate the mechanical response of nanobeams made of isotropic and/or composite materials, as briefly overviewed in the following.

In the field of nonlocal differential elasticity methodologies, Reddy [5] proposed some analytical solutions for the static, buckling, and vibration analyses of beams by considering different shear deformation theories. With the help of Eringen's non-local elasticity theory, deformation, instability, and vibrational analyses of the Euler-Bernoulli beam with variable geometrical and material properties were comprehensively inspected by Pradhan and Sarkar [6]. Similarly, Aydogdu [7] applied Eringen's elasticity model and different beam theories to derive a generalized nonlocal beam theory for the mechanical analysis of nano-size beams. A numerical formulation based on the differential quadrature method was proposed by Civalek and Akgöz [8] to study the free vibration characteristics of microtubules according to Eringen's non-local elasticity theory and Euler-Bernoulli beam hypotheses. Moreover, a modified couple stress theory was applied by Ke et al. [9], together with a first-order shear deformable beam model, to study the size-dependent dynamic stability of microbeams made from FGMs. Mohanty et al. [10], instead, applied the Timoshenko beam basics to study the statics and dynamics of simply supported beams made of transversely FGMs. Danesh et al. [11] obtained the motion equations for the longitudinal vibration of nanorods with tapered cross-sections and solved them via the differential quadrature method. To carry out the linear stability resistance of micro-columns with linearly varying cross-sections, Akgöz and Civalek [12] applied a Rayleigh-Ritz method. The surface impact on the nonlinear free vibration of elastically restrained non-local beams with variable cross-section was, also, examined by Malekzadeh and Shojaee [13]. In the further work by Ghannadpour et al. [14], the Ritz method was similarly employed to study the bending, buckling, and vibration of beams with arbitrary supports by assuming a nonlocal continuum theory. Through the strain gradient theory, Akgöz and Civalek [15] studied the instability of micro-beams with a material variation and subjected to various types of end supports. Among coupled problems, Ke and Wang [16] assessed the free vibrations of magneto-electro-elastic (MEE) nanobeams, based on a nonlocal theory and the Timoshenko beam model. At the same time, Rahmani and Pedram [17] adopted the nonlocal Timoshenko beam theory to exploit the size effect on the vibrational characteristics of nanobeams made of FGMs. In another research, the stability analysis of double nanobeam systems was carried out by Hosseini and Rahmani [18] in closed form, accounting for the surface effect via the theory of first-order shear deformation and nonlocal elasticity theory. Ebrahim et al. [19-22] performed some comprehensive investigations on the vibration and buckling response of nano-scale FG beams under different circumstances and through different beam theories. A novel numerical solution procedure was proposed by Fang and Zhou [23] including the Chebyshev polynomials and Ritz's method into to analyze the free vibration of rotating non-prismatic Timoshenko beams with a varying material from ceramic to metal in the axial direction. Different shear deformation beam theories were accomplished by Ghasemi and Mohandes [24-26] to study the free vibration behavior of multilayer composite beam whose equations of the problem were solved numerically according to the differential quadrature approach. Within the context of first-order shear deformation theory and von Kármán-type geometrical nonlinearity, Ansari and Gholami [27] explored the impact of small-scale sizes on the buckling and post-buckling strength of nanoplates subjected to a magneto-electro-thermo-mechanical loading condition. Pradhan and Chakraverty [28] considered six different patterns of the shear deformation to study the vibration of beams made of FGMs under different types of boundary conditions, while employing the Rayleigh-Ritz method to solve the problem. Following the nonlocal elasticity assumptions, Arefi and Zenkour [29] studied the impact of the mechanical, electrical and magnetic loads on the mechanical response of sandwich nanobeams. Chen and Chang [30] also performed a vibration analysis of FG beams with a rectangular section using a transformed-section approach and a first-order shear deformation beam model. For further numerical-based investigations on the bending, vibration, and buckling behaviors of nano-size structural elements made of different materials and subjected to various loadings, the reader is referred to [11, 14, 31-70]. In another study presented by Arefi [71], the mechanical response of laminated doubly curved nanoshells made of two piezoelectric layers and a homogeneous core loaded by a transverse electro-mechanical force was investigated in detail. Considering the effects of thermal environment, Jena et al. [72] proposed the Navier's method to study the buckling behavior of different types of Single Walled Carbon Nanotubes (SWNTs) lying on Winkler elastic foundation and subjected to simply supported end conditions. Soltani et al. [73, 74] applied the differential quadrature

method to assess the sustainable buckling load of axially FG nanobeams with a varying I-section, subjected to uniformly distributed load and/or compressive axial force. Moreover, in the context of different shear deformation patterns together with classical and/or nonlocal beam theories, several numerical studies about the static and dynamic analyses of nano-scale structures with different shapes and geometries exposed to different loading conditions can be found in Refs. [69, 75-87].

A literature review indicates that the stability behavior of nano-scale tapered Timoshenko beams with axially varying materials under compressive axial loading is usually governed by two differential equations coupled in terms of the vertical displacement and the rotation angle. Through different solution methodologies including numerical and/or analytical techniques, the endurable buckling of tapered AFG Timoshenko nanobeams has been investigated before by different authors. For instance, Ritz's method, the power series approximation and the differential quadrature method have been previously utilized to simulate the problem, as well as the finite element solution. Although such methods are capable of predicting the critical buckling loads with the desired precision, they need a considerable amount of time to be accomplished due to the simultaneous solution of a pair of differential equations. Based on these facts, the main objective of this paper is to introduce a simple approach for discussing the linear buckling behavior of nano-size first-order shear deformation beams with varying cross-sections as well as material properties, rather than solving the conventional system of non-local equilibrium equations. In this regard, the usually coupled differential equations for the mentioned beam element are thus condensed to a single equation. Indeed, the present approach is inspired by the easy-implementation mathematical approach, recently introduced by Soltani et al. [88, 89] for the buckling analysis of non-prismatic classical Timoshenko beams with axially varying materials.

Based on non-local elasticity theory and the Timoshenko beam model assumption, a pair of coupled equilibrium equations are first established using the energy principle for an axially compressed AFG tapered beam in the context of linear and elastic behavior. In the next step, the resulting two coupled differential equations with variable coefficients for the flexural displacement and the angle of rotation of the cross-section due to bending are reduced into a new single fifth-order differential equation, only in terms of the transverse displacement through the general and straightforward procedure suggested by Soltani et al. [88, 89]. As far as authors aware, the unique non-local equilibrium equation for buckling analysis AFG non-prismatic Timoshenko nanobeam has never been derived before. Owing to the presence of the variable coefficients in the resulting differential equation, the generalized differential equation is here employed for solving the equilibrium equation and calculating the critical loads. After verifying the accuracy and performances of the present procedure, a large numerical investigation checks for the impact of several essential parameters, such as the tapering ratio, nonlocal parameter, power-law exponent, and slenderness ratio, on the linear stability strength of size-dependent AFG Timoshenko beams with variable cross-sections, providing useful insights for further scientific investigations on the problem.

2. The equilibrium equations

Let consider an axially compressed non-prismatic straight beam element of length L whose height and width vary arbitrarily along the longitudinal direction (see Fig. 1). It is also assumed that the material properties of the beam with rectangular cross-section vary gradually in the axial direction. The orthogonal right-hand Cartesian coordinate system (x, y, z) is adopted, where x denotes the longitudinal axis and y and z refer to the first and second principal bending axes parallel to the width and thickness, respectively. The origin of these axes O is located at the centroid of the cross-section.

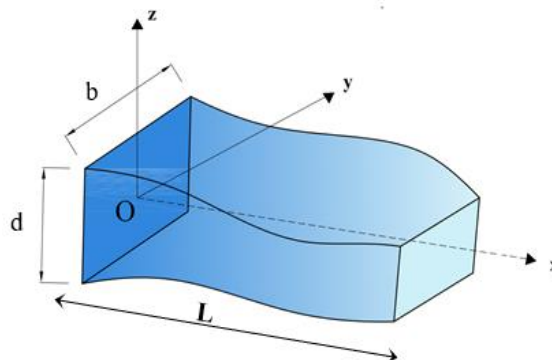


Fig. 1. Geometrical scheme for AFG Timoshenko beam with a non-uniform cross-section.

In this study, Timoshenko beam theory is applied to describe the displacement field of a point on the section contour. This classical theory contains the effects of rotary inertia, transverse shear deformation along with the flexural displacement. It is further admitted that the cross-section does not change any shape during deflection. Based on these assumptions and using a small displacement theory, the longitudinal and vertical displacement components, U and W , can be expressed as

$$U(x, y, z) = u_0(x) + z\theta(x) \quad (1a)$$

$$W(x, y, z) = w(x) \quad (1b)$$

where u_0 is the axial displacement at the midplane, which occurs only in presence of an external axial loading, w represents the vertical displacement (in z -direction), and θ is the angle of rotation of the cross-section due to bending. The Green's strain tensor components in large displacements, involving both the linear and non-linear strain parts are defined as

$$\varepsilon_{ij} = \frac{1}{2} \left(\frac{\partial U_i}{\partial x_j} + \frac{\partial U_j}{\partial x_i} \right) + \frac{1}{2} \left(\frac{\partial U_k}{\partial x_i} \frac{\partial U_k}{\partial x_j} \right) = \varepsilon_{ij}^l + \varepsilon_{ij}^* \quad i, j, k = x, y, z \quad (2)$$

where ε_{ij}^l and ε_{ij}^* stand for the linear and quadratic non-linear parts, respectively. Using the displacement field given in Eq. (1), the non-zero constituents of linear and non-linear parts of strain-displacement are derived as

$$\varepsilon_{xx}^l = \frac{\partial U}{\partial x} = u_0' + z\theta' \quad (3a)$$

$$\varepsilon_{xz}^l = \frac{1}{2} \left(\frac{\partial U}{\partial z} + \frac{\partial W}{\partial x} \right) = \frac{1}{2} (w' + \theta) \quad (3b)$$

$$\varepsilon_{xx}^* = \frac{1}{2} \left(\frac{\partial W}{\partial x} \right)^2 = \frac{1}{2} (w')^2 \quad (3c)$$

The resultants of classical stresses for Timoshenko beam can be expressed as follows [5]

$$N = \int_A \sigma_{xx} dA \quad (4a)$$

$$M = \int_A \sigma_{xx} z dA \quad (4b)$$

$$Q = \int_A \sigma_{xz} dA \quad (4c)$$

where N is the axial force applied at end member, M is the bending moments about major axis, Q is the shear force at any point of the beam, and σ_{ij} is the Piola–Kirchhoff stress tensor component.

As previously stated, for modelling the behavior of a non-scale element, the nonlocal elasticity theory introduced by Eringen is utilized in the current study. According to this theory [3], the stress at a point within a body depends not only on the strain state at that point but also on strain states at all other points throughout the body. For homogenous and isotropic elastic solids, the nonlocal stress tensor σ at point x can be thus defined as

$$\sigma_{ij}(x) = \int_V \alpha(|x' - x|, \tau) C_{ijkl} \varepsilon_{kl}^l(x') dV(x') \tag{5}$$

in which, ε_{kl}^l and C_{ijkl} denote the components of linear strain and elastic stiffness coefficients, respectively. Additionally, $\alpha(|x' - x|, \tau)$ refers to the nonlocal kernel function, and $|x' - x|$ is the Euclidean distance. In addition, the term $\tau = e_0 a/l$ stands for the material parameter, in which a is an internal characteristic length (e.g., lattice parameter, C–C bond length and granular distance), l represents an external characteristic length of the nanostructures (e.g., crack length, wavelength), as well as e_0 denotes a material constant which is determined experimentally or approximated by matching the dispersion curves of plane waves with those of atomic lattice dynamics. It is possible to express the integral constitutive equation presented in Eq. (5) in the form of the following differential constitutive equation

$$(1 - \mu \nabla^2) \sigma_{ij} = C_{ijkl} \varepsilon_{kl}^l \tag{6}$$

where ∇^2 is the Laplacian operator and $\mu = (e_0 a)^2$ denotes the non-local parameter. For Timoshenko nanobeams, the nonlocal stress-strain relations can be rewritten as [90]

$$\begin{Bmatrix} \sigma_{xx} \\ \sigma_{xz} \end{Bmatrix} - \mu \nabla^2 \begin{Bmatrix} \sigma_{xx} \\ \sigma_{xz} \end{Bmatrix} = \begin{bmatrix} E(x) & 0 \\ 0 & G(x) \end{bmatrix} \begin{Bmatrix} \varepsilon_{xx}^l \\ 2\varepsilon_{xz}^l \end{Bmatrix} \tag{7}$$

E and G are the elastic and shear moduli of the beam, respectively. Since the material properties vary arbitrarily in the longitudinal direction, the mentioned elastic properties are functions of the axial coordinate x , as

$$G(x) = \frac{E(x)}{2(1 + \nu)} \tag{8}$$

where ν is the Poisson’s ratio and maintains constant through the longitudinal direction [85, 86]. By substituting Eqs. (3a-b) into Eq. (8) and the subsequent results into Eq. (5), the nonlocal stress resultants are obtained as [5]

$$N - \mu \frac{\partial^2 N}{\partial x^2} = EA u_0' \tag{9a}$$

$$M - \mu \frac{\partial^2 M}{\partial x^2} = EI \theta' \tag{9b}$$

$$Q - \mu \frac{\partial^2 Q}{\partial x^2} = kGA (w' + \theta) \tag{9c}$$

In the previous expressions, k is the shear correction factor and assumed to be 5/6 for rectangular cross-section [5]. Moreover, A is the cross-section area, and I denotes the area moment of inertia about the y-axis which are defined as

$$(A, I) = \int_A (1, z^2) dA \tag{10}$$

In this research, the equilibrium equations and associated boundary conditions are derived from the stationary conditions of the total potential energy. Based on this principle, the following relation is considered:

$$\delta \Pi = \delta U_l + \delta U_0 - \delta W_e = 0 \tag{11}$$

In this formulation, δ denotes a variational operator, U_l and U_0 represent the elastic strain energy and the strain energy due to effects of the initial stresses, respectively. Also, W_e denotes the work done by the external loading applied on the structure. In the special case of the field of flexural stability, where the beam is not subjected to any external force, this parameter is equal to zero. In this context, δU_l can be computed using the following equation

$$\delta U_l = \int_V \sigma_{ij} \delta \varepsilon_{ij}^l dV = \int_0^L \int_A \sigma_{xx} \delta \varepsilon_{xx}^l dA dx + 2 \int_0^L \int_A \sigma_{xy} \delta \varepsilon_{xy}^l dA dx + 2 \int_0^L \int_A \sigma_{xz} \delta \varepsilon_{xz}^l dA dx \quad (12)$$

in which L expresses the element length, $\delta \varepsilon_{ij}^l$ is the variation of the linear parts of the strain tensor. Using the Eq. (3), the variation of the components of linear strain tensor is defined as

$$\delta \varepsilon_{xx}^l = \delta u_0' + z \delta \theta' \quad (13a)$$

$$\delta \varepsilon_{xz}^l = \frac{1}{2} (\delta w' + \delta \theta) \quad (13b)$$

$$\delta \varepsilon_{xy}^l = 0 \quad (13c)$$

Substituting Eqs. (13a-c) into Eq. (12) and integrating over the beam's cross-sectional area, the following expression is extracted:

$$\begin{aligned} \delta U_l &= \int_0^L \int_A \sigma_{xx} (\delta u_0 - z \delta \theta') dA dx + \int_0^L \int_A \sigma_{xz} (\delta w + \delta \theta') dA dx \\ &= \int_L (N \delta u_0' + M \delta \theta') dx + \int_L (Q (\delta w' + \delta \theta)) dx \end{aligned} \quad (14)$$

In addition, the variational form of the strain energy due to initial stresses is defined as

$$\delta U_0 = \int_V \sigma_{ij}^0 \delta \varepsilon_{ij}^* dV = \int_0^L \int_A \sigma_{xx}^0 \delta \varepsilon_{xx}^* dA dx + 2 \int_0^L \int_A \sigma_{xy}^0 \delta \varepsilon_{xy}^* dA dx + 2 \int_0^L \int_A \sigma_{xz}^0 \delta \varepsilon_{xz}^* dA dx \quad (15)$$

where σ_{xy}^0 and σ_{xz}^0 refer to the mean values of the shear stress and σ_{xx}^0 stands for the initial normal stress in the cross-section. In this study, the beam is initially subjected to an axial compression load P^0 acting at the end beam without any eccentricity. The most general case of the pre-buckling normal and shear stresses associated with the axial force applied at the beam supports P^0 are considered as

$$\sigma_{xx}^0 = \frac{P^0}{A}, \quad \sigma_{xz}^0 = \sigma_{xy}^0 = 0. \quad (16a, b)$$

Based on Eq. (3c), the first variation of non-linear strain-displacement relation can be written as

$$\delta \varepsilon_{xx}^* = w' \delta w' \quad (17)$$

In this stage, by substituting Eqs. (16) and (17) into Eq. (15), and integrating the expression over the cross-section area of the beam, the variation of strain energy due to the initial stresses takes the following form

$$\delta U_0 = \int_0^L \int_A \left(\frac{P^0}{A} \right) (w' \delta w') dA dx = \int_0^L P^0 (w' \delta w') dx \quad (18)$$

After combination of Eqs. (14), (18) into Eq. (11), the expression for the first variation of total potential energy can

be written as

$$\delta\Pi = \int_L (N \delta u_0' + M \delta\theta') dx + \int_L (Q(\delta w' + \delta\theta)) dx + \int_L (P^0(w' \delta w')) dx = 0 \quad (19)$$

By equating the coefficients of the virtual displacements ($\delta u_0, \delta w, \delta\theta$) to zero and integrating by parts, we obtain the following relations

$$-N' = 0 \quad (20a)$$

$$(P^0 w')' - Q' = 0 \quad (20b)$$

$$-M' + Q = 0 \quad (20c)$$

together with the following boundary conditions

$$N = 0 \quad \text{Or} \quad \delta u_0 = 0 \quad (21a)$$

$$-P^0 w' + Q = 0 \quad \text{Or} \quad \delta w = 0 \quad (21b)$$

$$M = 0 \quad \text{Or} \quad \delta\theta = 0 \quad (21c)$$

By substituting the nonlocal resultant components (Eq. (9)) into Eq. (20), the final equilibrium equations in terms of primary displacement field are obtained as follows

$$\delta u_0 : (EAu_0')' = 0 \quad (22a)$$

$$\delta w : (kGA(w' + \theta))' - Pw'' + \mu Pw^{iv} = 0 \quad (22b)$$

$$\delta\theta : (EI\theta')' - kGA(w' + \theta) = 0 \quad (22c)$$

The boundary conditions of the beam can be also expressed as

$$N = 0 \quad \text{Or} \quad \delta u_0 = 0$$

$$kGA(w' + \theta) - Pw' + \mu Pw''' = 0 \quad \text{Or} \quad \delta w = 0 \quad (23)$$

$$EI\theta' + \mu Pw'' = 0 \quad \text{Or} \quad \delta\theta = 0$$

In these differential equations, the successive x -derivatives are denoted by $(\bullet)'$, $(\bullet)''$. In this stage, it is important to note that the 1st differential equation Eq. (22a) is uncoupled and does not affect the linear stability analysis of an elastic nanobeam subjected to compressive axial load. As in presence of axial force P^0 , the rotation of the cross-section θ , as well as the vertical displacement w , the two other equilibrium equations (22b-c) have a coupled structure.

Based on the straightforward methodology presented by Soltani et al. [88, 89], the governing equilibrium equation

for the vertical displacement (22b) can be rewritten as

$$\theta = \frac{-\mu P w''' + (P - kGA) w'}{kGA} \quad (24)$$

whose substitution in the third equilibrium Eq. (22c) enables its redefinition in an uncoupled form just dependent on the deflection w , independently from the rotation θ , i.e.

$$\left(\frac{EI}{(kGA)^2} ((kGA)(-\mu P w''' + (P - kGA) w') - (kGA)'(-\mu P w''' + (P - kGA) w')) \right)' + \mu P w''' - P w' = 0 \quad (25)$$

By setting the nonlocality parameter μ equal to zero, the following formulations in the context of the classical beam theory are obtained in line with the equilibrium equations by Soltani et al. [88, 89]

$$\left(\frac{EI}{(kGA)^2} ((kGA)((P - kGA) w') - (kGA)'((P - kGA) w')) \right)' - P w' = 0 \quad (26)$$

or equivalently [82, 83]

$$(kGA)(EI \theta')' + P(kGA \theta - (EI \theta')) = 0 \quad (27)$$

Based on the authors' knowledge, the resulting single fifth-order differential equation for stability analysis of AFG Timoshenko nanobeam having non-uniform cross-section has not been acquired previously. Due to the uncoupling the system of equilibrium equations, the formula developed herein could simplify the essential computational effort to calculate the critical axial load. Therefore, the execution time of the analysis is reduced and the procedure can be accomplished with low computational cost.

In the current work, the geometric and material properties can vary arbitrarily in the axial direction, and consequently, all stiffness quantities of the AFG tapered Timoshenko nanobeam are functions of the x -coordinate. Accordingly, the closed-form solution of the resulting fifth-order differential equation in function of the section rotation (25) is not straightforward, but required some numerical procedures.

3. Solution Methodology

In this section, the numerical solution of a resulting fifth-order differential equation is developed. Thus, the Generalized Differential Quadrature Method (GDQM) is here employed to calculate the axial critical loading. This methodology is based on the approximation of a derivative of a function at a specified point by the sum of the weighted factors and the values of the function at any set points in the problem-solving range. According to GDQM, the r^{th} order derivative of a function $f(x)$ at an arbitrary point is described as [91, 92]

$$\left. \frac{d^r f}{dx^r} \right|_{x=x_p} = \sum_{j=1}^N A_{ij}^{(r)} f(x_j) \quad \text{for } i = 1, 2, \dots, N \quad (28)$$

where N is the number of grid points along the x direction; x_j refers to the position of each sample point and $f(x_j)$ is the corresponding function value. Moreover, $A_{ij}^{(r)}$ denotes the weighting coefficient for the r^{th} - order derivative. The first-order derivative weighting coefficient ($A_{ij}^{(1)}$) is computed by the following algebraic formulations which are based on Lagrangian interpolation polynomials

$$A_{ij}^{(1)} = \begin{cases} \frac{M(\xi_i)}{(\xi_i - \xi_j)M(\xi_j)} & \text{for } i \neq j \\ -\sum_{k=1, k \neq i}^N A_{ik}^{(1)} & \text{for } i=j \end{cases} \quad i, j = 1, 2, \dots, N \quad (29)$$

where

$$M(\xi_i) = \prod_{j=1, j \neq i}^N (\xi_i - \xi_j) \quad \text{for } i = 1, 2, \dots, N \quad (30)$$

The higher-order GDQM weighting coefficients can be computed from the first-order weighting coefficient as

$$A_{ij}^{(r)} = A_{ij}^{(1)} A_{ij}^{(r-1)} \quad 2 \leq r \leq N - 1 \quad (31)$$

In this study, a Chebyshev–Gauss–Lobatto discretization is used to define the position of each sample point [93]

$$x_i = \frac{L}{2} \left[1 - \cos\left(\frac{i-1}{N-1} \pi\right) \right], \quad (32)$$

if $0 \leq x \leq L \quad i = 1, 2, \dots, N$

To simplify the numerical solution procedure of the equilibrium equation utilizing the GDQM, a non-dimensional variable ($\xi = x / L$) is adopted. Thus, the final stability equation (25) and Eq. (32) can be transformed into the following non-dimensional form

$$\begin{aligned} & -P \mu EI (kGA)^2 \left(\frac{d^5 w}{d \xi^5}\right) + 2P \mu EI (kGA) \left(\frac{d(kGA)}{d \xi}\right) \left(\frac{d^4 w}{d \xi^4}\right) - P \mu (kGA)^2 \left(\frac{dEI}{d \xi}\right) \left(\frac{d^4 w}{d \xi^4}\right) \\ & + P \mu EI (kGA) \left(\frac{d^2 kGA}{d \xi^2}\right) \left(\frac{d^3 w}{d \xi^3}\right) - 2P \mu EI \left(\frac{d(kGA)}{d \xi}\right)^2 \left(\frac{d^3 w}{d \xi^3}\right) + P \mu (kGA) \left(\frac{dEI}{d \xi}\right) \left(\frac{d(kGA)}{d \xi}\right) \left(\frac{d^3 w}{d \xi^3}\right) \\ & + P \mu L^2 (kGA)^3 \left(\frac{d^3 w}{d \xi^3}\right) - L^2 EI (kGA)^3 \left(\frac{d^3 w}{d \xi^3}\right) + PL^2 EI (kGA)^2 \left(\frac{d^3 w}{d \xi^3}\right) \\ & - 2PL^2 EI (kGA) \left(\frac{d(kGA)}{d \xi}\right) \left(\frac{d^2 w}{d \xi^2}\right) - L^2 (kGA)^3 \left(\frac{dEI}{d \xi}\right) \left(\frac{d^2 w}{d \xi^2}\right) + PL^2 (kGA)^2 \left(\frac{dEI}{d \xi}\right) \left(\frac{d^2 w}{d \xi^2}\right) \\ & - PL^2 EI (kGA) \left(\frac{d^2(kGA)}{d \xi^2}\right) \left(\frac{dw}{d \xi}\right) + 2PL^2 EI \left(\frac{d(kGA)}{d \xi}\right)^2 \left(\frac{dw}{d \xi}\right) \\ & - PL^2 (kGA) \left(\frac{dEI}{d \xi}\right) \left(\frac{d(kGA)}{d \xi}\right) \left(\frac{dw}{d \xi}\right) - PL^4 (kGA)^3 \left(\frac{dw}{d \xi}\right) = 0 \end{aligned} \quad (33a)$$

$$\xi_i = \frac{1}{2} \left[1 - \cos\left(\frac{i-1}{N-1} \pi\right) \right], \quad \text{if } 0 \leq \xi \leq 1 \quad i = 1, 2, \dots, N \quad (33b)$$

By applying the differential quadrature discretization to the non-dimensional governing Eq. (33b) leads to the following expression

$$\begin{aligned}
& \left\{ -P \mu (E(\xi_j) I(\xi_j)) (kG(\xi_j) A(\xi_j))^2 \right\} \left(\sum A_{ij}^{(5)} w_j \right) \\
& + \left\{ \begin{aligned} & 2P \mu (E(\xi_j) I(\xi_j)) (kG(\xi_j) A(\xi_j)) (kG'(\xi_j) A(\xi_j) + kG(\xi_j) A'(\xi_j)) \\ & - P \mu (E'(\xi_j) I(\xi_j) + E(\xi_j) I'(\xi_j)) (kG(\xi_j) A(\xi_j))^2 \end{aligned} \right\} \left(\sum A_{ij}^{(4)} w_j \right) \\
& + \left\{ \begin{aligned} & P \mu (E(\xi_j) I(\xi_j)) (kG(\xi_j) A(\xi_j)) (kG''(\xi_j) A(\xi_j) + kG(\xi_j) A''(\xi_j) + 2kG'(\xi_j) A'(\xi_j)) \\ & - 2P \mu (E(\xi_j) I(\xi_j)) (kG'(\xi_j) A(\xi_j) + kG(\xi_j) A'(\xi_j))^2 \\ & + P \mu (kG(\xi_j) A(\xi_j)) (E'(\xi_j) I(\xi_j) + E(\xi_j) I'(\xi_j)) (kG'(\xi_j) A(\xi_j) + kG(\xi_j) A'(\xi_j)) \\ & + P \mu L^2 (kG(\xi_j) A(\xi_j))^3 - L^2 (E(\xi_j) I(\xi_j)) (kG(\xi_j) A(\xi_j))^3 \\ & + PL^2 (E(\xi_j) I(\xi_j)) (kG(\xi_j) A(\xi_j))^2 \end{aligned} \right\} \left(\sum A_{ij}^{(3)} w_j \right) \\
& + \left\{ \begin{aligned} & -2PL^2 (E(\xi_j) I(\xi_j)) (kG(\xi_j) A(\xi_j)) (kG'(\xi_j) A(\xi_j) + kG(\xi_j) A'(\xi_j)) \\ & - L^2 (kG(\xi_j) A(\xi_j))^3 (E'(\xi_j) I(\xi_j) + E(\xi_j) I'(\xi_j)) \\ & + PL^2 (kG(\xi_j) A(\xi_j))^2 (E'(\xi_j) I(\xi_j) + E(\xi_j) I'(\xi_j)) \end{aligned} \right\} \left(\sum A_{ij}^{(2)} w_j \right) \\
& + \left\{ \begin{aligned} & -PL^2 (E(\xi_j) I(\xi_j)) (kG(\xi_j) A(\xi_j)) (kG''(\xi_j) A(\xi_j) + kG(\xi_j) A''(\xi_j) + 2kG'(\xi_j) A'(\xi_j)) \\ & + 2PL^2 (E(\xi_j) I(\xi_j)) (kG'(\xi_j) A(\xi_j) + kG(\xi_j) A'(\xi_j))^2 - PL^4 (kG(\xi_j) A(\xi_j))^3 \\ & - PL^2 (kG(\xi_j) A(\xi_j)) (E'(\xi_j) I(\xi_j) + E(\xi_j) I'(\xi_j)) (kG'(\xi_j) A(\xi_j) + kG(\xi_j) A'(\xi_j)) \end{aligned} \right\} \left(\sum A_{ij}^{(1)} w_j \right) = 0
\end{aligned} \tag{34}$$

The matrix form of the resulting formulation can be written as

$$\begin{aligned}
& P \mu [a][A]^5 \{w\} + P \mu ([b] + [c])[A]^4 \{w\} \\
& + (P \mu ([d] + [e] + [f] + [g]) - PL^2 [a] + [h])[A]^3 \{w\} \\
& + ([i] - PL^2 ([b] + [c]))[A]^2 \{w\} + (-PL^2 ([d] + [e] + [f] + [g]))[A]^1 \{w\} = 0
\end{aligned} \tag{35}$$

in which

$$\begin{aligned}
a_{jk} &= (-EI)(kGA)^2 \Big|_{\xi=\xi_j} \delta_{jk}; \quad b_{jk} = (2EI)(kGA)(kGA' + kG'A) \Big|_{\xi=\xi_j} \delta_{jk} \\
c_{jk} &= (-kGA)^2 (EI' + E'I) \Big|_{\xi=\xi_j} \delta_{jk}; \quad d_{jk} = (EI)(kG''A + kG'A'' + 2kG'A') \Big|_{\xi=\xi_j} \delta_{jk} \\
e_{jk} &= (-2EI)(kGA' + kG'A)^2 \Big|_{\xi=\xi_j} \delta_{jk}; \quad f_{jk} = (kGA)(EI' + E'I)(kGA' + kG'A) \Big|_{\xi=\xi_j} \delta_{jk} \\
g_{jk} &= (L^2(kGA)^3) \Big|_{\xi=\xi_j} \delta_{jk}; \quad h_{jk} = (-L^2(EI)(kGA)^3) \Big|_{\xi=\xi_j} \delta_{jk}; \quad i_{jk} = (-L^2(kGA)^3(EI' + E'I)) \Big|_{\xi=\xi_j} \delta_{jk}
\end{aligned} \tag{36a}$$

$$\{w\} = \{w(\xi_1) \quad w(\xi_2) \quad w(\xi_3) \quad \dots \quad w(\xi_n)\} \tag{36b}$$

and δ_{jk} is Kronecker delta function.

The simple form of the resulting expression (Eq. (35)) can be stated as

$$\left([K^*] + P[K_G] \right) \{w\} = 0 \tag{37}$$

in which

$$\begin{aligned}
 [K_G] &= \mu[a][A]^5 + \mu([b]+[c])[A]^{(4)} + (\mu([d]+[e]+[f]+[g]) - L^2[a])[A]^{(3)} \\
 &\quad - L^2([b]+[c])[A]^{(2)} - L^2([d]+[e]+[f]+[g])[A]^{(1)} \\
 [K^*] &= [h][A]^{(3)} + [i][A]^{(2)}
 \end{aligned}
 \tag{38}$$

$[K_G]$ and $[K^*]$ are $N \times N$ matrices. As mentioned previously, N denotes the number of grid points along the computation domain ($0 \leq \xi \leq 1$). In this research study, the numerical solutions for a simply supported nanobeam are obtained using the differential quadrature technique. The corresponding boundary conditions of a simply supported Timoshenko nanobeam can be expressed as

$$\begin{aligned}
 \left. \begin{aligned}
 &\xi = 0 \\
 &\text{and} \\
 &\xi = 1
 \end{aligned} \right\} \begin{aligned}
 &-\mu PEI(kGA) \frac{d^4 w}{d\xi^4} + \mu PEI \frac{d(kGA)}{d\xi} \frac{d^3 w}{d\xi^3} + \mu PL^2(kGA)^2 \frac{d^2 w}{d\xi^2} \\
 &+ PL^2 EI(kGA) \frac{d^2 w}{d\xi^2} - EIL^2(kGA)^2 \frac{d^2 w}{d\xi^2} - PEIL^2 \frac{d(kGA)}{d\xi} \frac{dw}{d\xi} = 0
 \end{aligned} \tag{39a, b} \\
 &w = 0
 \end{aligned}$$

After accomplishment associated boundary conditions of a simply supported given by Eq. (39), the buckling load for nanotapered Timoshenko beams with axially varying materials along with the vertical deformation is derived using the eigenvalue solution of Eq. (37).

4. Numerical results and discussions

This section explores the effect of different predominant parameters such as FG power index, aspect ratio, non-locality parameter, and tapering ratios on the linear buckling strength of simply supported AFG double-tapered nanobeams based on the first-order shear deformation theory. Both tabular and graphical outcomes are illustrated in this context. We utilize the subscripts of $()_0$ and $()_1$ to represent the mechanical specifications including the material and geometrical ones of the beam element at the left support ($x=0, \xi=0$) and the right one ($x=L, \xi=1$), respectively. Through this example, the linear buckling analysis is performed for a simply supported width and thickness tapered Timoshenko beam under a concentrated compressive axial load. In this regard, it is supposed that the width (b_0) and the height (d_0) of the rectangular profile at the left end vary linearly to $b_1 = (1 + \beta)b_0$ and $d_1 = (1 + \alpha)d_0$ at the right side. Therefore, the rates of cross-section change along the width and thickness are defined as $\beta = b_1/b_0 - 1$ and $\alpha = d_1/d_0 - 1$, respectively; α is the height and β is the width tapering ratio, respectively, which can vary in the range of $-0.9 \leq \alpha, \beta$. This means that the width and thickness increase by increasing the tapering ratios for all positive values $0 < \alpha, \beta$. Additionally, the width and thickness of the rectangular profile decrease linearly when the tapering parameters are negative $-0.9 \leq \alpha, \beta < 0$. Note that by equating these two mentioned parameters (α, β) to zero, a prismatic Timoshenko beam is achieved. Moreover, the non-uniformity parameters (α, β) can change concurrently or separately. In this benchmark example, it is also considered that the beam is made of axially varying materials. The material properties vary along the beam length from a pure ceramic at the left end to a pure metal at the right one using a simple power-law function. Hence, the modulus of elasticity in the local coordinate is expressed as [94, 95]

$$E(x) = E_0 + (E_1 - E_0) \left(\frac{x}{L}\right)^m \tag{40}$$

It should be stated that the power-law index m , is a positive parameter and by setting it equals zero, the beam becomes a fully metal member. Moreover, the following non-dimensional expression is used in the figures and tables

$$P_{nor} = \frac{P_{cr} L^2}{E_0 I_0} \tag{41}$$

in which A_0 and I_0 represent the cross-sectional area and moment of inertia at the left support, respectively, defined as $I_0 = b_0 d_0^3 / 12$ and $A_0 = b_0 d_0$.

The current part is divided in two different subsections; the first one checks for the convergence and verification of the formulation proposed herein, and the latter aims to peruse the influence of the above-mentioned factors on the linear buckling behavior of the considered member.

4.1. Convergence of DQ methodology

The aim of the first section of the current example is to define the minimum number of sampling points along the longitudinal direction while using the methodology of differential quadrature employed herein, to obtain accurate results. To this end, we consider an AFG double tapered beam with the following parameters: $E_0 = 200GPa$, $E_1 = 70GPa$, $L/b_0 = 20$. The lowest values of the non-dimensional axial load of the selected nano-tapered Timoshenko beam with a fixed Eringen’s parameter ($\mu = 2.0$) and two different tapering ratios ($\beta = \alpha = 0.2$, and 0.8) by setting the power-law index m equal to one, are evaluated versus the number of sampling points adopted in DQ methodology and the outcomes are presented in Fig. 2.

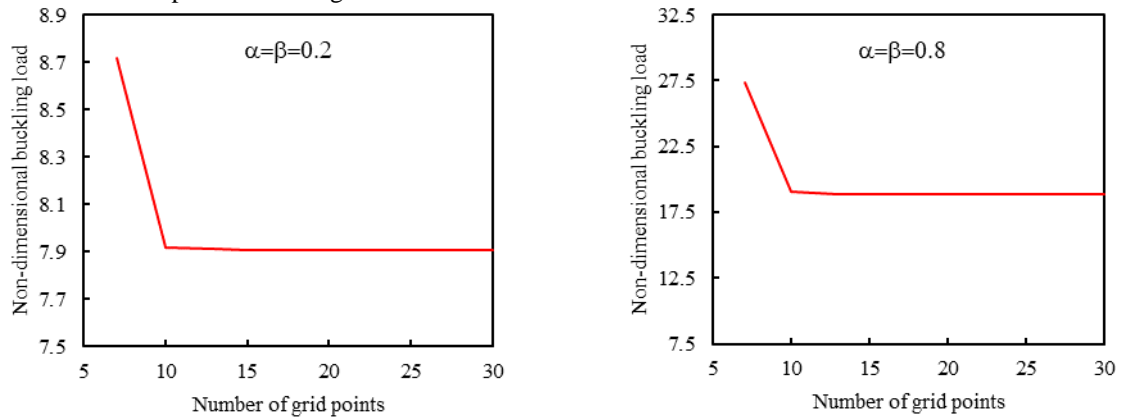


Fig. 2. Normalized buckling load of a nanotapered AFG beam vs. the number of grid points.

It is visible from Fig. 2 that by increasing the number of points N from 15 to 20, the predicted buckling load tends to converge. In the following computations, we take $N = 20$ to calculate the first buckling loads, unless otherwise stated.

4.2. Verification

After performing the convergence studies, it turns to investigate the accuracy and validity of the developed formulation in the present work. Thus, the validation of the developed procedure for buckling analysis of simply supported AFG tapered Timoshenko beam in the context of classical elasticity theory is checked by comparing our results with predictions by Soltani et al. [88] and Shahba et al. [96]. Once again, it is assumed that the FG beam is made of Zirconium dioxide (ZrO_2) and Aluminium (Al) with the following properties (ZrO_2 : $E_0=200GPa$; Al: $E_1=70GPa$). The other corresponding geometric parameters are: $L=1$, $I_0/A_0 = 0.01$, $m=1$. Non-dimensional buckling loads assessed using the GDQM with 20 grid points are illustrated in Table 1 for different negative values of height and width tapering parameters (α, β). In this section, two different types of variation in the cross-section profile are considered, namely, a thickness tapered beam, and a double-tapered beam.

Table 1. Variation of the normalized buckling loads of AFG tapered local beam with the tapering ratios and different FG power-exponents.

Variation of cross-section	m=1				m=3			
	Tapering parameter	Present	Ref. [96]	$\Delta(\%)$	Tapering parameter	Present	Ref. [88]	$\Delta(\%)$
Thickness tapered beam	$\beta=0, \alpha=-0.9$	4.7422	4.7632	0.4409	$\beta=0, \alpha=-0.8$	4.2483	4.434	4.1881
	$\beta=0, \alpha=-0.7$	4.0066	4.0176	0.2738	$\beta=0, \alpha=-0.6$	2.8736	2.9396	2.2452
	$\beta=0, \alpha=-0.5$	3.3050	3.3093	0.1299	$\beta=0, \alpha=-0.4$	1.6339	1.6461	0.7411
	$\beta=0, \alpha=-0.3$	2.6436	2.6439	0.0113	$\beta=0, \alpha=-0.2$	0.6462	0.6266	3.1344
Double tapered	$\alpha=\beta=-0.9$	4.4276	4.4532	0.5746	$\alpha=\beta=-0.8$	3.6184	3.8388	5.7414

beam	$\alpha=\beta=-0.7$	3.4570	3.4735	0.4749	$\alpha=\beta=-0.6$	1.9896	2.0824	4.4564
	$\alpha=\beta=-0.5$	2.6020	2.6104	0.3199	$\alpha=\beta=-0.4$	0.8459	0.8649	2.2003
	$\alpha=\beta=-0.3$	1.8686	1.8702	0.0881	$\alpha=\beta=-0.2$	0.2105	0.1937	8.6526

Table 1 shows that the critical load values computed using the proposed technique are in good agreement with the results from [88, 96] so that the error rate is less than 10%. The efficiency and performance of the proposed solution are, thus, confirmed.

In the next step, to validate the analysis in the context of nonlocal elasticity theory, the estimated results by the suggested formula for simply supported homogenous Timoshenko nanobeams with uniform cross-sections are compared with [5]. The numerical outcomes for non-dimensional buckling loads are listed in Table 2 for different slenderness ratios $L/b_0=10$, $L/b_0=20$, and $L/b_0=100$. To make the comparison possible, the corresponding parameters are: $L=10$, $E=30 \times 10^6$, $\nu=0.3$.

Table 2. Variation of the dimensionless buckling load of homogenous prismatic Timoshenko beam with simply supported end conditions for different slenderness ratios (L/b_0).

μ	$L/b_0=10$		$L/b_0=20$		$L/b_0=100$	
	Reddy [5]	Present	Reddy [5]	Present	Reddy [5]	Present
0.0	9.6228	9.6228	9.8067	9.8067	9.8671	9.8671
0.5	9.1701	9.1701	9.3455	9.3455	9.4031	9.4031
1	8.7583	8.7583	8.9258	8.9258	8.9807	8.9807
1.5	8.3818	8.3818	8.5421	8.5421	8.5947	8.5947
2.0	8.0364	8.0364	8.1900	8.19	8.2405	8.2405
2.5	7.7183	7.7183	7.8659	7.8659	7.9143	7.9143
3.0	7.4244	7.4244	7.5664	7.5664	7.613	7.613
3.5	7.1521	7.1521	7.2889	7.2889	7.3337	7.3337
4.0	6.899	6.899	7.0310	7.031	7.0743	7.0743
4.5	6.6633	6.6633	6.7907	6.7907	6.8325	6.8325
5.0	6.4431	6.4431	6.5663	6.5663	6.6068	6.6068

It is observed that the employed numerical methodology of solution in the current study gives the same results as the analytical ones reported in [5].

4.3. Parametric Study

After the validation step, an exhaustive parametric investigation is now performed to assess the sensitivity of the linear buckling strength to various key parameters such as in-homogeneous index, nonlocal parameter, slenderness ratio and thickness and breadth tapering parameters. Note that in this section, the ceramic-metal FG nanoscale beam is made of Alumina (Al_2O_3) and Aluminium (Al) with the following properties (Al_2O_3 : $E_0=380GPa$; Al : $E_1=70GPa$). Based on the suggested approach, the normalized critical loads of simply supported nanoscale tapered AFG beam with a fixed aspect ratio ($L/b_0=20$) for various values of tapering ratios (i.e. $\alpha = \beta = 0, 0.3, 0.6, 0.9$), FG power-law indices, and five different nonlocal parameters are listed in Table 3. In this case, the values of Eringen’s nonlocality parameter are taken as 0, 1, 2, 3, 4 nm^2 . Note that the compressive axial load is located at the beam extremities without any eccentricity.

Table 3. Effect of the tapering parameter and material composition on the dimensionless buckling load of simply supported nano-size Timoshenko beams with $L/b_0=20$ under a compressive axial load with five different nonlocal parameters.

Material composition		Nonlocal parameters				
		$\mu=0$	$\mu=1$	$\mu=2$	$\mu=3$	$\mu=4$
m=0.7	0.0	4.3093	3.8547	3.4826	3.1746	2.9169
	0.3	5.3863	4.8366	4.3824	4.0029	3.6828
	0.6	6.6120	5.9562	5.4106	4.9512	4.5605
	0.9	7.9940	7.2228	6.5790	6.0344	5.5687
m=3.0	0.0	8.0668	7.2686	6.5792	5.9729	5.4355
	0.3	9.9447	8.9986	8.2030	7.5252	6.9424

	0.6	12.0218	10.9030	9.9724	9.1871	8.5165
	0.9	14.2977	12.9769	11.8815	10.9580	10.1685
Homogeneous (Alumina)	0.0	9.8067	8.9258	8.1900	7.5664	7.0310
	0.3	16.5361	14.9764	13.6731	12.5676	11.6179
	0.6	19.1607	17.2959	15.7367	14.4133	13.2756
	0.9	21.9744	19.7572	17.9018	16.3255	14.9697

Next, in Figs. 3-5 we plot the influence of nonlocality parameters (varying in the range between 0 and 4) on the variations of normalized buckling loads of ceramic-metal functionally graded double tapered beam with respect to non-uniformity parameters (ranging from 0 to 1) with different power-law exponents, respectively for $L/b_0 = 10$, $L/b_0 = 50$, and $L/b_0 = 100$. In this stage, the nano-tapered Timoshenko beam having equal thickness and breadth tapering ratios ($\alpha=\beta$) is perused.

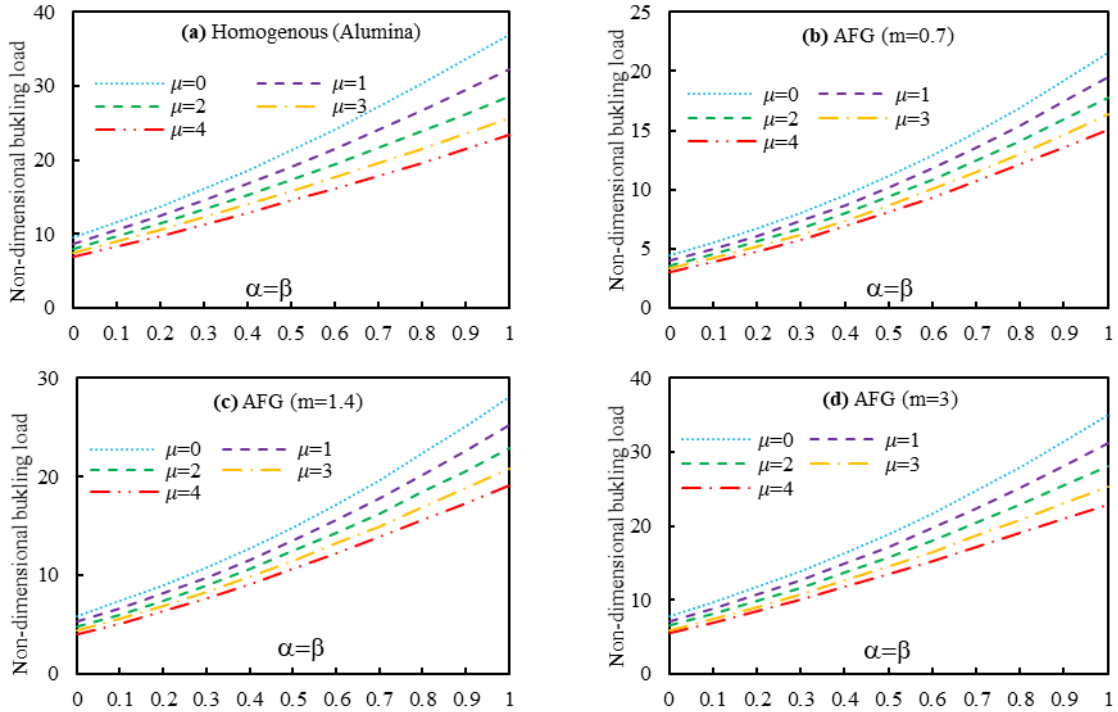
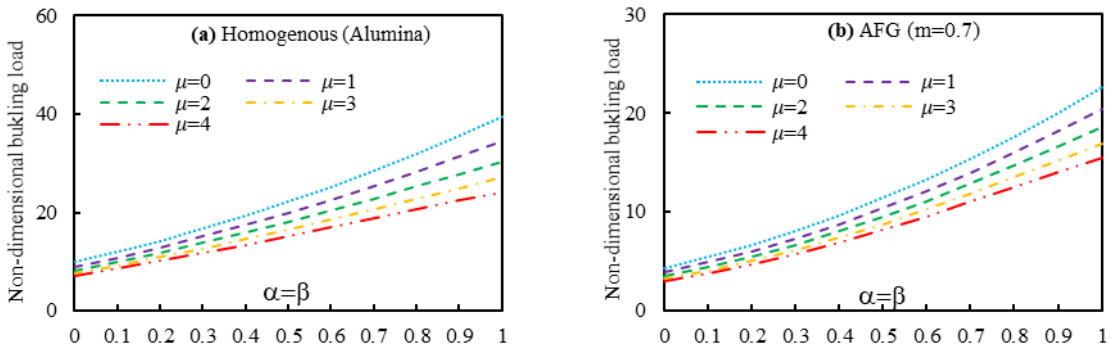


Fig. 3. Variation of the non-dimensional buckling load for nano-tapered Timoshenko beams with the tapering and nonlocality parameters for different material indexes ($L/b_0=10$): (a) Homogeneous (Alumina); (b) $m=0.7$; (c) $m=1.4$; (d) $m=3$.



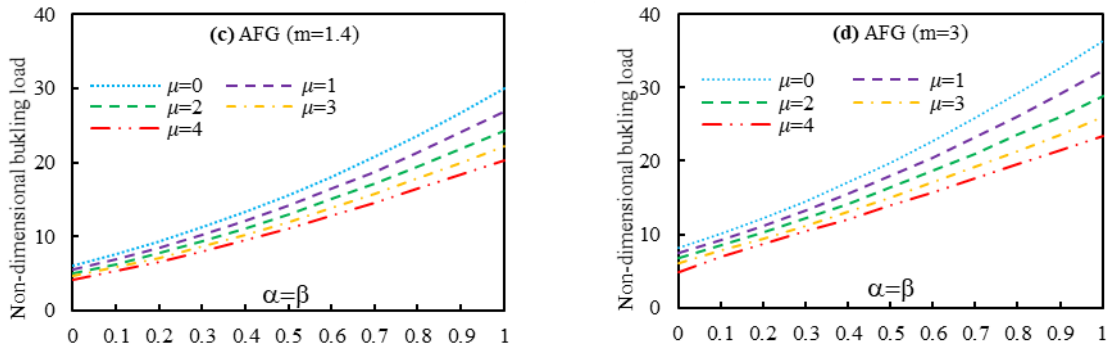


Fig. 4. Variation of the non-dimensional buckling load of nano-tapered Timoshenko beams with the tapering and nonlocality parameters for different material indexes ($L/b_0=50$): (a) Homogeneous (Alumina); (b) $m=0.7$; (c) $m=1.4$; (d) $m=3$.

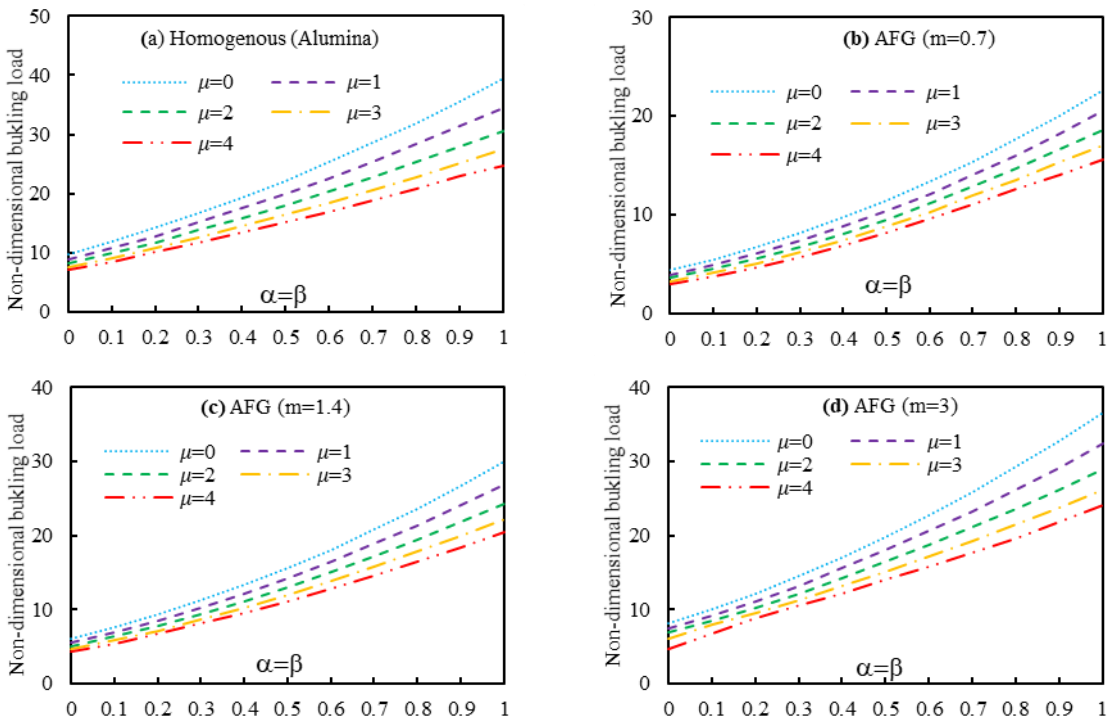


Fig. 5. Variation of the non-dimensional buckling load of nanotapered Timoshenko beams with the tapering and nonlocality parameters for different material indexes ($L/b_0=100$): (a) Homogenous (Alumina); (b) $m=0.7$; (c) $m=1.4$; (d) $m=3$.

Also, the lowest axial buckling load parameters of nano-size double-tapered FG Timoshenko beams with $L/b_0=50$ are reported Table 4 to check for the effect of power-law indices, nonlocal parameters, and non-uniformity ratio on the stability resistance of the considered nanoscale beam element.

Table 4. Lowest buckling parameters of Timoshenko nanobeam with fixed $L/b_0=50$ and different power-law indices (m), tapering ratios, and nonlocality parameter.

Nonlocal parameters	$\alpha = \beta$	Material composition					
		$m=0.5$	$m=1$	$m=1.5$	$m=2$	$m=2.5$	$m=3$
$\mu=0$	0.0	3.9245	5.3073	6.3244	7.0872	7.6640	8.1032
	0.3	4.8873	6.6258	7.8826	8.8078	9.4945	10.0083
	0.6	5.9722	8.1112	9.6315	10.7305	11.5320	12.1215
	0.9	7.1823	9.7670	11.5735	12.8569	13.7769	14.4430

$\mu=1$	0.0	3.5401	4.7739	5.6892	6.3829	6.9129	7.3200
	0.3	4.4270	5.9912	7.1299	7.9745	8.6053	9.0794
	0.6	5.4242	7.3593	8.7410	9.7443	10.4777	11.0175
	0.9	6.5332	8.8790	10.5221	11.6904	12.5268	13.1304
$\mu=2$	0.0	3.2189	4.3255	5.1516	5.7844	6.2737	6.6539
	0.3	4.0424	5.4593	6.4970	7.2728	7.8566	8.2979
	0.6	4.9664	6.7301	7.9950	8.9178	9.5944	10.0930
	0.9	5.9910	8.1368	9.6429	10.7150	11.4815	12.0330
$\mu=3$	0.0	2.9463	3.9414	4.6860	5.2615	5.7130	6.0697
	0.3	3.7162	5.0061	5.9550	6.6701	7.2132	7.6271
	0.6	4.5781	6.1954	7.3599	8.2136	8.8421	9.3061
	0.9	5.5312	7.5070	8.8964	9.8866	10.5940	11.1014

Similarly, Figs. 6-8 are devoted to show the impact of FG power-law exponent and Eringen’s nonlocal parameter (i.e. $\mu = 0, 1, 2, 3 \text{ nm}^2$) on the buckling strength of the selected axially compressed nanoscale beam with respect to variations of tapering parameter, under the assumption $\alpha = \beta$, and for different aspect ratios. Each figure shows six different plots relating to $m=0.5, 1, 1.5, 2, 2.5$ and 3 .

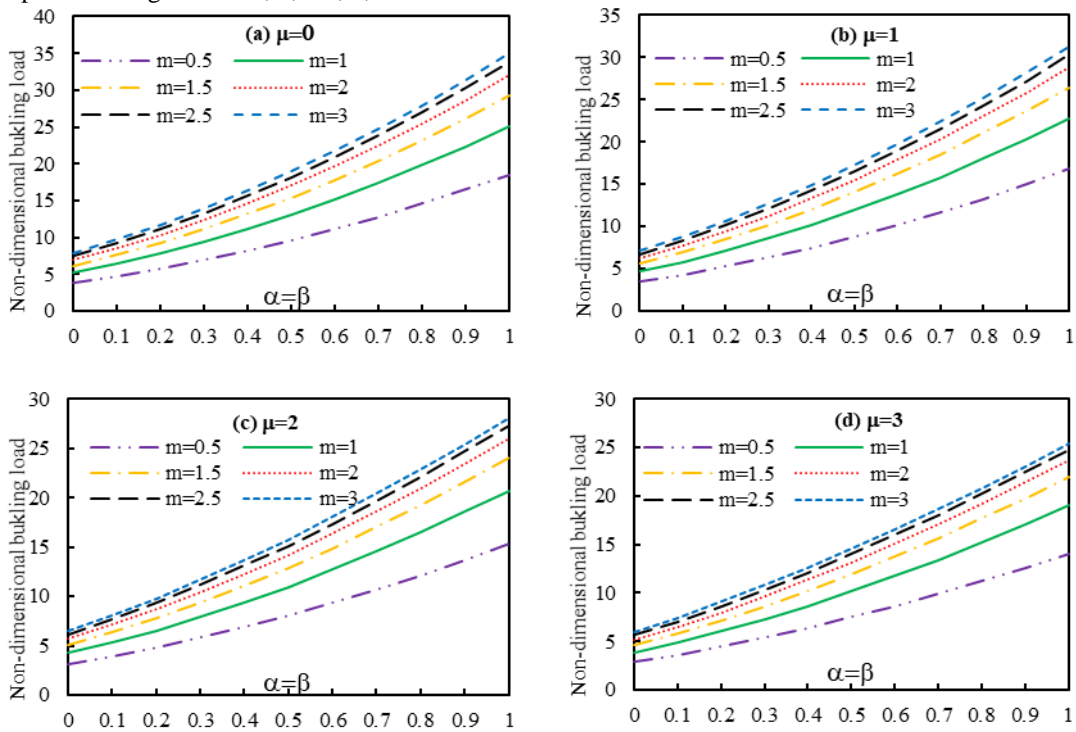


Fig. 6. Variation of the non-dimensional buckling load of nano-tapered Timoshenko beams with the tapering and material indexes for different nonlocality parameters ($L/b_0=10$): (a) $\mu=0$; (b) $\mu=1$; (c) $\mu=2$; (d) $\mu=3$.

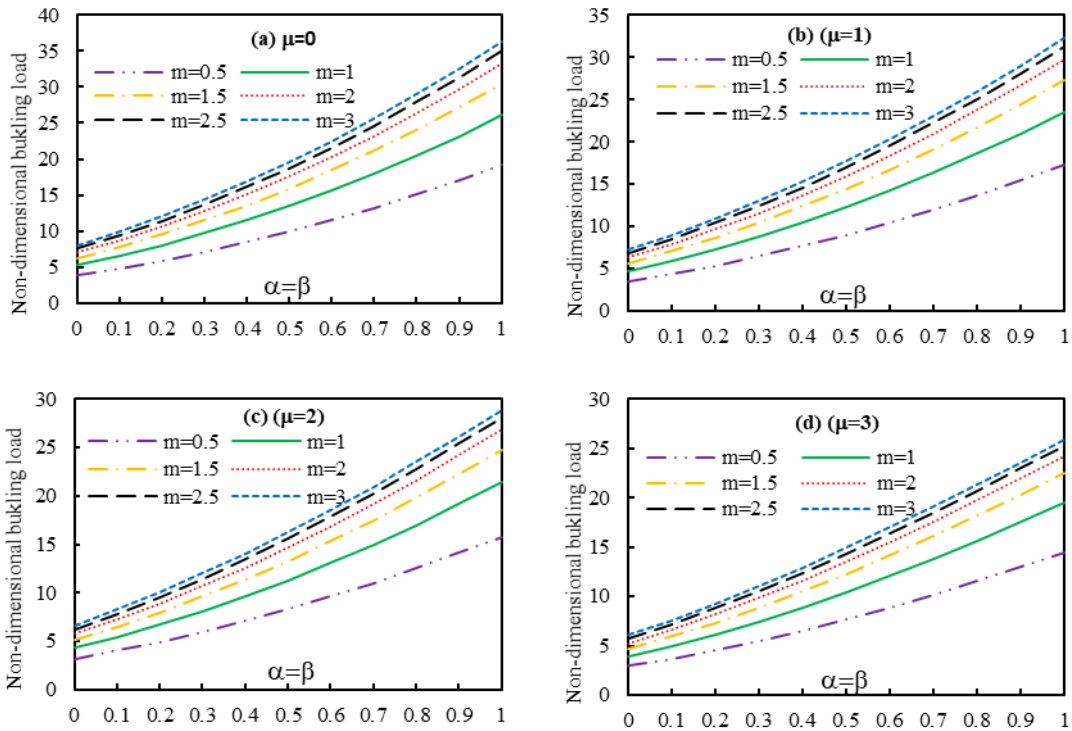


Fig. 7. Variation of the non-dimensional buckling load of nano-tapered Timoshenko beams with the tapering and material indexes for different nonlocality parameters ($L/b_0=20$): (a) $\mu=0$; (b) $\mu=1$; (c) $\mu=2$; (d) $\mu=3$.

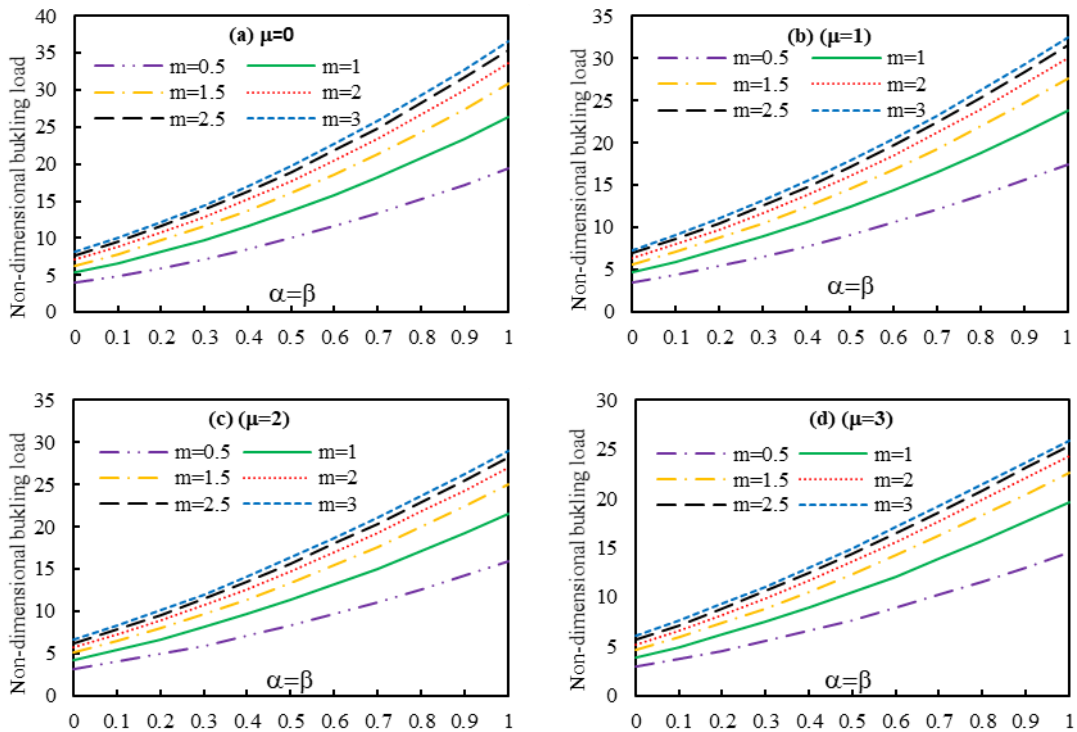


Fig. 8. Variation of the non-dimensional buckling load of nano-tapered Timoshenko beams with the tapering and material indexes for different nonlocality parameters ($L/b_0=100$): (a) $\mu=0$; (b) $\mu=1$; (c) $\mu=2$; (d) $\mu=3$.

In addition, Fig. 9 shows the influence of simultaneous variations of width and height tapering ratios (α, β), Eringen's parameters ($\mu = 0, 1$ and $3, \text{nm}^2$), and two different aspect ratios ($L/b_0 = 10$, and 100) on the endurable buckling load of the homogeneous nano-tapered beam in the context of first-order shear deformation theory.

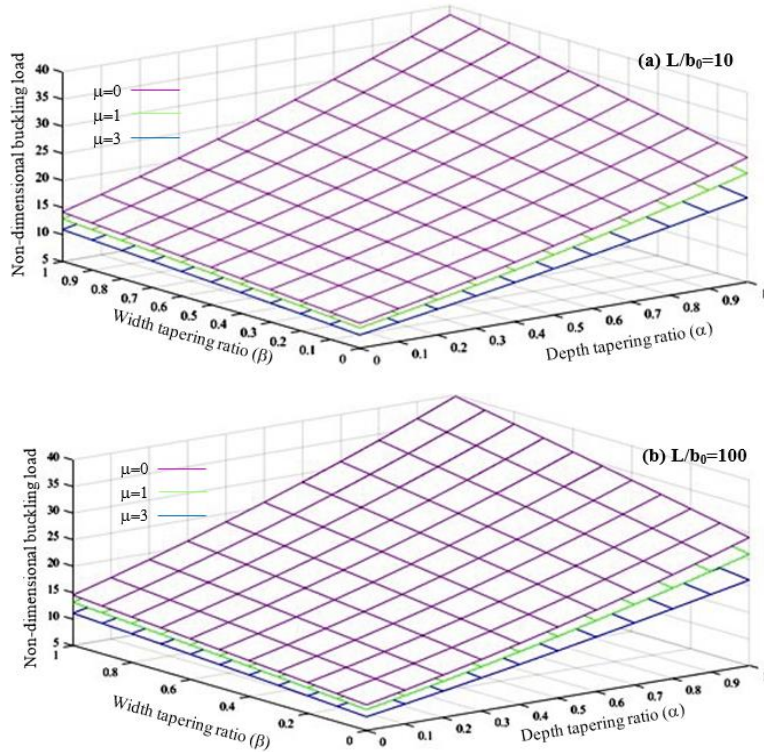
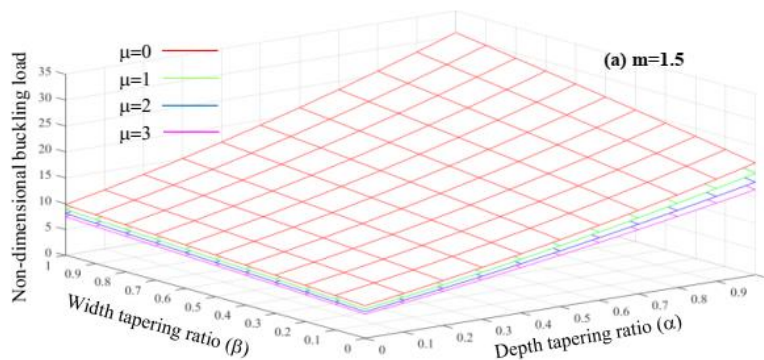


Fig. 9. Variation of the non-dimensional buckling load of homogeneous nano-tapered Timoshenko beams for various depth and width tapering ratios and different Eringen's parameters: (a) $L/b_0 = 10$; (b) $L/b_0 = 100$

Graphical results are presented in Fig. 10 where the variation of non-dimensional buckling loads of ceramic-metal FG nanoscale double tapered beam at constant slenderness ratio $L/b_0 = 50$ with respect to width and thickness tapering parameters (α, β) for different non-locality parameters ($\mu = 0, 1, 2$ and 3 nm^2) and gradient indices ($m = 1.5$, and 3) is investigated.



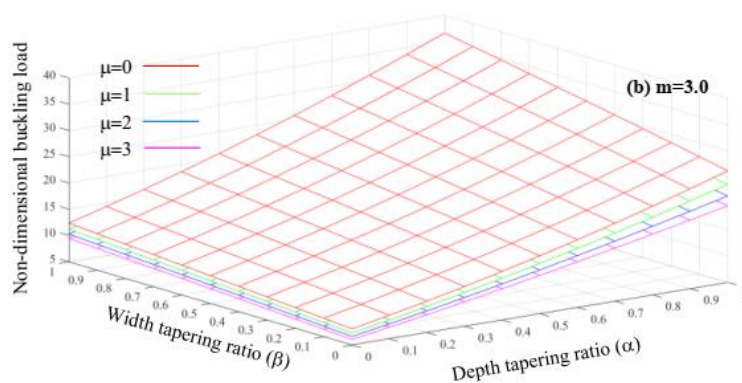


Fig. 10. Variation of the non-dimensional buckling load of AFG nano-tapered Timoshenko beams for various depth and width tapering ratios and different Eringen's parameters: (a) $m=1.5$; (b) $m=3.0$.

The tables and figures indicate that non-uniformity parameters have a considerable impact on the dimensionless buckling load. The negative tapering parameter weakens the nano-tapered beam due to the decreased geometrical characteristics including the cross-sectional area and moment of inertia, while the other results relating the positive tapering ratios do not follow a similar pattern. In other words, the linear stability strength is enhanced for an increased tapering ratio. This sensitivity of the response is more noticeable for depth tapering parameter (α), while becoming even more insignificant for the breadth tapering parameter (β). The reason is attributed to the fact that the first buckling mode shape occurs with respect to the minor axis moment of inertia. This could yield a different beneficial effect on the overall structural response of many nano-engineering components such as nonuniform scanning tunnelling microscopes, oscillators or sensors

It can be seen that with the increase in FG power exponent, the material features continuously change from alumina to Aluminum, and as a result, the bending stiffness of the nano-scale beam increases greatly, yielding a higher buckling capacity. One can also conclude that with the increment of power-law index m , the endurable critical load increases obviously for $0.5 \leq m \leq 1.5$. For greater values of in-homogeneous index $m > 1.5$, the stability strength increases slightly.

As observed in the above illustrations and tables, it is noticed that the dimensionless critical load is enhanced by increasing the slenderness ratio. This means that the shear deformation loses its impact on the total deflections, as the value of the slenderness ratio increases. In other words, by eliminating the transverse shear deformation, the stability of the nanoscale structure is improved.

It is concluded that the non-dimensional buckling loads decrease significantly with the increase of the nonlocality parameter related to Eringen's nonlocal elasticity theory. For the cases considered in Table 3, the axial buckling parameter (P_{nor}) of double-tapered ceramic-metal FG beam with $\alpha=\beta=0.6$ and $m=3.0$ decreases approximately 30%, when μ increases from 0 to 4. This statement can be explained by the fact that the bending stiffness, as well as the shear stiffness, of the tapered Timoshenko beam in the nanoscale, are inversely proportional to Eringen's parameter. In general, the inclusion of the nonlocal effect increases the deflection, which in turn leads to a decrease in the member's stiffness quantity, resulting in a weaker member. Since the linear buckling resistance of beam is proportional to the stiffness of the member, a significant reduction in the critical load of the beam is observed. This confirms the findings from the literature, for which classical formulations overestimate the results compared to nonlocal formulations.

5. Conclusions

In this paper, a simple and novel method is introduced for discussing the linear stability strength of AFC nanoscale beams with varying cross-sections in the context of the first-order shear deformation theory. The Eringen nonlocal elasticity theory and the energy method are employed to establish a system of two-coupled differential equations in terms of the flexural displacement and the angle of rotation due to bending. In the next stage, the obtained coupled fourth-order governing differential equations are transformed into a fifth-order order differential equation with variable coefficients only in terms of the vertical deflection. The GDQM is here adopted as efficient numerical strategy to solve the resulting equation, and to compute the critical buckling load. To show the exactness of the present methodology, the obtained results have been compared to those ones based on classical elasticity theory and nonlocal elasticity from literature. Subsequently, the impact of thickness and/or width tapering ratios, FG power exponent, nonlocal parameter and slenderness ratio on buckling capacity of simply supported Timoshenko tapered nanobeam

with axially varying materials has been exhaustively surveyed through a parametric study. Besides the outcomes presented in the text, the following remarks can be expressed:

- By comparing the attained outcomes with the exciting exact results, the fast convergence and effectiveness of the suggested approach are confirmed.
- It is believed that the methodology proposed herein facilitates the stability analysis of axially loaded AFG nano-tapered Timoshenko beams, and represents a very efficient way to reduce the computational effort.
- The proposed formulation is comprehensive and feasible and could proceed with various practical problems dealing with different types of variation in material and geometric properties of the cross-section profile along the longitudinal direction.
- For the whole cases analysed herein, it is found that the stability strength decreases as the nonlocality parameter gets larger, whereas the endurable buckling load increases as ceramic phase increases.
- It can also be stated that the effects of linear variation in the width and height of rectangular cross-section play noticeable roles on the linear stability strength of tapered Timoshenko nanobeam.
- Finally, it can be concluded that AFG Timoshenko nanobeams with nonuniform cross-section feature some engineering characteristics that can be controlled in accordance with the gradient index, non-uniformity parameter along with the aspect ratio. Engineers can thus design small-scale structural elements with favorable stability and optimal distribution of strength and weight.

References

- [1] F. Yang, A. Chong, D. Lam, P. Tong, Couple stress based strain gradient theory for elasticity, *International journal of solids and structures*, Vol. 39, No. 10, pp. 2731-2743, 2002.
- [2] M. E. Gurtin, J. Weissmüller, F. Larche, A general theory of curved deformable interfaces in solids at equilibrium, *Philosophical Magazine A*, Vol. 78, No. 5, pp. 1093-1109, 1998.
- [3] A. C. Eringen, Nonlocal polar elastic continua, *International journal of engineering science*, Vol. 10, No. 1, pp. 1-16, 1972.
- [4] A. Eringen, On differential equations of nonlocal elasticity and solutions of screw dislocation and surface waves, *Journal of applied physics*, Vol. 54, No. 9, pp. 4703-4710, 1983.
- [5] J. Reddy, Nonlocal theories for bending, buckling and vibration of beams, *International journal of engineering science*, Vol. 45, No. 2-8, pp. 288-307, 2007.
- [6] S. Pradhan, A. Sarkar, Analyses of tapered FGM beams with nonlocal theory, *Structural Engineering and Mechanics, An Int'l Journal*, Vol. 32, No. 6, pp. 811-833, 2009.
- [7] M. Aydogdu, A general nonlocal beam theory: its application to nanobeam bending, buckling and vibration, *Physica E: Low-dimensional Systems and Nanostructures*, Vol. 41, No. 9, pp. 1651-1655, 2009.
- [8] O. Civalek, B. Akgöz, Free vibration analysis of microtubules as cytoskeleton components: nonlocal Euler-Bernoulli beam modeling, 2010.
- [9] L.-L. Ke, Y.-S. Wang, Size effect on dynamic stability of functionally graded microbeams based on a modified couple stress theory, *Composite Structures*, Vol. 93, No. 2, pp. 342-350, 2011.
- [10] S. Mohanty, R. Dash, T. Rout, Static and dynamic stability analysis of a functionally graded Timoshenko beam, *International Journal of Structural Stability and Dynamics*, Vol. 12, No. 04, pp. 1250025, 2012.
- [11] M. Danesh, A. Farajpour, M. Mohammadi, Axial vibration analysis of a tapered nanorod based on nonlocal elasticity theory and differential quadrature method, *Mechanics Research Communications*, Vol. 39, No. 1, pp. 23-27, 2012.
- [12] B. Akgöz, Ö. mer Civalek, Buckling analysis of linearly tapered micro-columns based on strain gradient elasticity, *Structural Engineering and Mechanics, An Int'l Journal*, Vol. 48, No. 2, pp. 195-205, 2013.
- [13] P. Malekzadeh, M. Shojaee, Surface and nonlocal effects on the nonlinear free vibration of non-uniform nanobeams, *Composites Part B: Engineering*, Vol. 52, pp. 84-92, 2013.
- [14] S. Ghannadpour, B. Mohammadi, J. Fazilati, Bending, buckling and vibration problems of nonlocal Euler beams using Ritz method, *Composite Structures*, Vol. 96, pp. 584-589, 2013.
- [15] B. Akgöz, Ö. Civalek, Buckling analysis of functionally graded microbeams based on the strain gradient theory, *Acta Mechanica*, Vol. 224, No. 9, pp. 2185-2201, 2013.
- [16] L.-L. Ke, Y.-S. Wang, Free vibration of size-dependent magneto-electro-elastic nanobeams based on the nonlocal theory, *Physica E: Low-Dimensional Systems and Nanostructures*, Vol. 63, pp. 52-61, 2014.
- [17] O. Rahmani, O. Pedram, Analysis and modeling the size effect on vibration of functionally graded nanobeams based on nonlocal Timoshenko beam theory, *International Journal of Engineering Science*, Vol. 77, pp. 55-70, 2014.

- [18] S. Hosseini, O. Rahmani, Surface effects on buckling of double nanobeam system based on nonlocal Timoshenko model, *International Journal of Structural Stability and Dynamics*, Vol. 16, No. 10, pp. 1550077, 2016.
- [19] F. Ebrahimi, M. Reza Barati, Vibration analysis of nonlocal beams made of functionally graded material in thermal environment, *The European Physical Journal Plus*, Vol. 131, pp. 1-22, 2016.
- [20] F. Ebrahimi, G. R. Shaghghi, M. Boreiry, A semi-analytical evaluation of surface and nonlocal effects on buckling and vibrational characteristics of nanotubes with various boundary conditions, *International Journal of Structural Stability and Dynamics*, Vol. 16, No. 06, pp. 1550023, 2016.
- [21] F. Ebrahimi, M. R. Barati, Buckling analysis of nonlocal third-order shear deformable functionally graded piezoelectric nanobeams embedded in elastic medium, *Journal of the Brazilian Society of Mechanical Sciences and Engineering*, Vol. 39, pp. 937-952, 2017.
- [22] F. Ebrahimi, M. R. Barati, A nonlocal strain gradient refined beam model for buckling analysis of size-dependent shear-deformable curved FG nanobeams, *Composite Structures*, Vol. 159, pp. 174-182, 2017.
- [23] J.-S. Fang, D. Zhou, Free vibration analysis of rotating axially functionally graded tapered Timoshenko beams, *International Journal of Structural Stability and Dynamics*, Vol. 16, No. 05, pp. 1550007, 2016.
- [24] M. Mohandes, A. R. Ghasemi, Finite strain analysis of nonlinear vibrations of symmetric laminated composite Timoshenko beams using generalized differential quadrature method, *Journal of Vibration and Control*, Vol. 22, No. 4, pp. 940-954, 2016.
- [25] A. Ghasemi, M. Mohandes, Nonlinear free vibration of laminated composite Euler-Bernoulli beams based on finite strain using generalized differential quadrature method, *Mechanics of Advanced Materials and Structures*, Vol. 24, No. 11, pp. 917-923, 2017.
- [26] M. Mohandes, A. R. Ghasemi, Modified couple stress theory and finite strain assumption for nonlinear free vibration and bending of micro/nanolaminated composite Euler–Bernoulli beam under thermal loading, *Proceedings of the Institution of Mechanical Engineers, Part C: Journal of Mechanical Engineering Science*, Vol. 231, No. 21, pp. 4044-4056, 2017.
- [27] R. Ansari, R. Gholami, Size-dependent buckling and postbuckling analyses of first-order shear deformable magneto-electro-thermo elastic nanoplates based on the nonlocal elasticity theory, *International Journal of Structural Stability and Dynamics*, Vol. 17, No. 01, pp. 1750014, 2017.
- [28] K. K. Pradhan, S. Chakraverty, Natural frequencies of shear deformed functionally graded beams using inverse trigonometric functions, *Journal of the Brazilian Society of Mechanical Sciences and Engineering*, Vol. 39, pp. 3295-3313, 2017.
- [29] M. Arefi, A. M. Zenkour, Size-dependent vibration and bending analyses of the piezomagnetic three-layer nanobeams, *Applied Physics A*, Vol. 123, pp. 1-13, 2017.
- [30] W.-R. Chen, H. Chang, Vibration analysis of functionally graded Timoshenko beams, *International Journal of Structural Stability and Dynamics*, Vol. 18, No. 01, pp. 1850007, 2018.
- [31] M. Mohammadi, A. Rastgoo, Primary and secondary resonance analysis of FG/lipid nanoplate with considering porosity distribution based on a nonlinear elastic medium, *Mechanics of Advanced Materials and Structures*, Vol. 27, No. 20, pp. 1709-1730, 2020.
- [32] M. Mohammadi, M. Hosseini, M. Shishesaz, A. Hadi, A. Rastgoo, Primary and secondary resonance analysis of porous functionally graded nanobeam resting on a nonlinear foundation subjected to mechanical and electrical loads, *European Journal of Mechanics-A/Solids*, Vol. 77, pp. 103793, 2019.
- [33] M. Mohammadi, A. Rastgoo, Nonlinear vibration analysis of the viscoelastic composite nanoplate with three directionally imperfect porous FG core, *Structural Engineering and Mechanics, An Int'l Journal*, Vol. 69, No. 2, pp. 131-143, 2019.
- [34] A. Farajpour, A. Rastgoo, M. Mohammadi, Vibration, buckling and smart control of microtubules using piezoelectric nanoshells under electric voltage in thermal environment, *Physica B: Condensed Matter*, Vol. 509, pp. 100-114, 2017.
- [35] A. Farajpour, M. H. Yazdi, A. Rastgoo, M. Loghmani, M. Mohammadi, Nonlocal nonlinear plate model for large amplitude vibration of magneto-electro-elastic nanoplates, *Composite Structures*, Vol. 140, pp. 323-336, 2016.
- [36] A. Farajpour, M. H. Yazdi, A. Rastgoo, M. Mohammadi, A higher-order nonlocal strain gradient plate model for buckling of orthotropic nanoplates in thermal environment, *Acta Mechanica*, Vol. 227, pp. 1849-1867, 2016.
- [37] M. Mohammadi, M. Safarabadi, A. Rastgoo, A. Farajpour, Hygro-mechanical vibration analysis of a rotating viscoelastic nanobeam embedded in a visco-Pasternak elastic medium and in a nonlinear thermal environment, *Acta Mechanica*, Vol. 227, pp. 2207-2232, 2016.

- [38] M. R. Farajpour, A. Rastgoo, A. Farajpour, M. Mohammadi, Vibration of piezoelectric nanofilm-based electromechanical sensors via higher-order non-local strain gradient theory, *Micro & Nano Letters*, Vol. 11, No. 6, pp. 302-307, 2016.
- [39] M. Baghani, M. Mohammadi, A. Farajpour, Dynamic and stability analysis of the rotating nanobeam in a nonuniform magnetic field considering the surface energy, *International Journal of Applied Mechanics*, Vol. 8, No. 04, pp. 1650048, 2016.
- [40] M. Goodarzi, M. Mohammadi, M. Khooran, F. Saadi, Thermo-mechanical vibration analysis of FG circular and annular nanoplate based on the visco-pasternak foundation, *Journal of Solid Mechanics*, Vol. 8, No. 4, pp. 788-805, 2016.
- [41] H. Asemi, S. Asemi, A. Farajpour, M. Mohammadi, Nanoscale mass detection based on vibrating piezoelectric ultrathin films under thermo-electro-mechanical loads, *Physica E: Low-dimensional Systems and Nanostructures*, Vol. 68, pp. 112-122, 2015.
- [42] M. Safarabadi, M. Mohammadi, A. Farajpour, M. Goodarzi, Effect of surface energy on the vibration analysis of rotating nanobeam, 2015.
- [43] M. Goodarzi, M. Mohammadi, A. Gharib, Techno-Economic Analysis of Solar Energy for Cathodic Protection of Oil and Gas Buried Pipelines in Southwestern of Iran, in *Proceeding of*, [https://publications.waset.org/abstracts/33008/techno-economic-analysis-of ...](https://publications.waset.org/abstracts/33008/techno-economic-analysis-of-...), pp.
- [44] M. Mohammadi, A. A. Nekounam, M. Amiri, The vibration analysis of the composite natural gas pipelines in the nonlinear thermal and humidity environment, in *Proceeding of*, <https://civilica.com/doc/540946/>, pp.
- [45] M. Goodarzi, M. Mohammadi, M. Rezaee, Technical Feasibility Analysis of PV Water Pumping System in Khuzestan Province-Iran, in *Proceeding of*, [https://publications.waset.org/abstracts/18930/technical-feasibility ...](https://publications.waset.org/abstracts/18930/technical-feasibility-...), pp.
- [46] M. Mohammadi, A. Farajpour, A. Moradi, M. Ghayour, Shear buckling of orthotropic rectangular graphene sheet embedded in an elastic medium in thermal environment, *Composites Part B: Engineering*, Vol. 56, pp. 629-637, 2014.
- [47] M. Mohammadi, A. Moradi, M. Ghayour, A. Farajpour, Exact solution for thermo-mechanical vibration of orthotropic mono-layer graphene sheet embedded in an elastic medium, *Latin American Journal of Solids and Structures*, Vol. 11, pp. 437-458, 2014.
- [48] M. Mohammadi, A. Farajpour, M. Goodarzi, F. Dinari, Thermo-mechanical vibration analysis of annular and circular graphene sheet embedded in an elastic medium, *Latin American Journal of Solids and Structures*, Vol. 11, pp. 659-682, 2014.
- [49] M. Mohammadi, A. Farajpour, M. Goodarzi, Numerical study of the effect of shear in-plane load on the vibration analysis of graphene sheet embedded in an elastic medium, *Computational Materials Science*, Vol. 82, pp. 510-520, 2014.
- [50] A. Farajpour, A. Rastgoo, M. Mohammadi, Surface effects on the mechanical characteristics of microtubule networks in living cells, *Mechanics Research Communications*, Vol. 57, pp. 18-26, 2014.
- [51] S. R. Asemi, M. Mohammadi, A. Farajpour, A study on the nonlinear stability of orthotropic single-layered graphene sheet based on nonlocal elasticity theory, *Latin American Journal of Solids and Structures*, Vol. 11, pp. 1541-1546, 2014.
- [52] M. Goodarzi, M. Mohammadi, A. Farajpour, M. Khooran, Investigation of the effect of pre-stressed on vibration frequency of rectangular nanoplate based on a visco-Pasternak foundation, 2014.
- [53] S. Asemi, A. Farajpour, H. Asemi, M. Mohammadi, Influence of initial stress on the vibration of double-piezoelectric-nanoplate systems with various boundary conditions using DQM, *Physica E: Low-dimensional Systems and Nanostructures*, Vol. 63, pp. 169-179, 2014.
- [54] S. Asemi, A. Farajpour, M. Mohammadi, Nonlinear vibration analysis of piezoelectric nanoelectromechanical resonators based on nonlocal elasticity theory, *Composite Structures*, Vol. 116, pp. 703-712, 2014.
- [55] M. Mohammadi, M. Ghayour, A. Farajpour, Free transverse vibration analysis of circular and annular graphene sheets with various boundary conditions using the nonlocal continuum plate model, *Composites Part B: Engineering*, Vol. 45, No. 1, pp. 32-42, 2013.
- [56] M. Mohammadi, M. Goodarzi, M. Ghayour, A. Farajpour, Influence of in-plane pre-load on the vibration frequency of circular graphene sheet via nonlocal continuum theory, *Composites Part B: Engineering*, Vol. 51, pp. 121-129, 2013.
- [57] M. Mohammadi, A. Farajpour, M. Goodarzi, R. Heydarshenas, Levy type solution for nonlocal thermo-mechanical vibration of orthotropic mono-layer graphene sheet embedded in an elastic medium, *Journal of Solid Mechanics*, Vol. 5, No. 2, pp. 116-132, 2013.

- [58] M. Mohammadi, A. Farajpour, M. Goodarzi, H. Mohammadi, Temperature Effect on Vibration Analysis of Annular Graphene Sheet Embedded on Visco-Pasternak Foundati, *Journal of Solid Mechanics*, Vol. 5, No. 3, pp. 305-323, 2013.
- [59] A. Farajpour, A. Shahidi, M. Mohammadi, M. Mahzoon, Buckling of orthotropic micro/nanoscale plates under linearly varying in-plane load via nonlocal continuum mechanics, *Composite Structures*, Vol. 94, No. 5, pp. 1605-1615, 2012.
- [60] M. Mohammadi, M. Goodarzi, M. Ghayour, S. Alivand, Small scale effect on the vibration of orthotropic plates embedded in an elastic medium and under biaxial in-plane pre-load via nonlocal elasticity theory, 2012.
- [61] A. Farajpour, M. Mohammadi, A. Shahidi, M. Mahzoon, Axisymmetric buckling of the circular graphene sheets with the nonlocal continuum plate model, *Physica E: Low-dimensional Systems and Nanostructures*, Vol. 43, No. 10, pp. 1820-1825, 2011.
- [62] A. Farajpour, M. Danesh, M. Mohammadi, Buckling analysis of variable thickness nanoplates using nonlocal continuum mechanics, *Physica E: Low-dimensional Systems and Nanostructures*, Vol. 44, No. 3, pp. 719-727, 2011.
- [63] H. Moosavi, M. Mohammadi, A. Farajpour, S. Shahidi, Vibration analysis of nanorings using nonlocal continuum mechanics and shear deformable ring theory, *Physica E: Low-dimensional Systems and Nanostructures*, Vol. 44, No. 1, pp. 135-140, 2011.
- [64] M. Mohammadi, M. Ghayour, A. Farajpour, Analysis of free vibration sector plate based on elastic medium by using new version differential quadrature method, *Journal of solid mechanics in engineering*, Vol. 3, No. 2, pp. 47-56, 2011.
- [65] A. Farajpour, M. Mohammadi, M. Ghayour, Shear buckling of rectangular nanoplates embedded in elastic medium based on nonlocal elasticity theory, in *Proceeding of*, www.civilica.com/Paper-ISME19-ISME19_390.html, pp. 390.
- [66] M. Mohammadi, A. Farajpour, A. R. Shahidi, Higher order shear deformation theory for the buckling of orthotropic rectangular nanoplates using nonlocal elasticity, in *Proceeding of*, www.civilica.com/Paper-ISME19-ISME19_391.html, pp. 391.
- [67] M. Mohammadi, A. Farajpour, A. R. Shahidi, Effects of boundary conditions on the buckling of single-layered graphene sheets based on nonlocal elasticity, in *Proceeding of*, www.civilica.com/Paper-ISME19-ISME19_382.html, pp. 382.
- [68] M. Mohammadi, M. Ghayour, A. Farajpour, Using of new version integral differential method to analysis of free vibration orthotropic sector plate based on elastic medium, in *Proceeding of*, www.civilica.com/Paper-ISME19-ISME19_497.html, pp. 497.
- [69] M. Mohammadi, A. Farajpour, A. Moradi, M. Hosseini, Vibration analysis of the rotating multilayer piezoelectric Timoshenko nanobeam, *Engineering Analysis with Boundary Elements*, Vol. 145, pp. 117-131, 2022.
- [70] M. Mohammadi, A. Farajpour, A. Rastgoo, Coriolis effects on the thermo-mechanical vibration analysis of the rotating multilayer piezoelectric nanobeam, *Acta Mechanica*, Vol. 234, No. 2, pp. 751-774, 2023/02/01, 2023.
- [71] M. Arefi, Size-dependent electro-elastic analysis of a three-layered piezoelectric doubly curved nano shell, *Mechanics of Advanced Materials and Structures*, Vol. 27, No. 23, pp. 1945-1965, 2020.
- [72] S. K. Jena, S. Chakraverty, M. Malikan, F. Tornabene, Stability analysis of single-walled carbon nanotubes embedded in winkler foundation placed in a thermal environment considering the surface effect using a new refined beam theory, *Mechanics Based Design of Structures and Machines*, Vol. 49, No. 4, pp. 581-595, 2021.
- [73] M. Soltani, F. Atoufi, F. Mohri, R. Dimitri, F. Tornabene, Nonlocal elasticity theory for lateral stability analysis of tapered thin-walled nanobeams with axially varying materials, *Thin-Walled Structures*, Vol. 159, pp. 107268, 2021.
- [74] M. Soltani, F. Atoufi, F. Mohri, R. Dimitri, F. Tornabene, Nonlocal analysis of the flexural-torsional stability for FG tapered thin-walled beam-columns, *Nanomaterials*, Vol. 11, No. 8, pp. 1936, 2021.
- [75] M. Karimi, K. Khorshidi, R. Dimitri, F. Tornabene, Size-dependent hydroelastic vibration of FG microplates partially in contact with a fluid, *Composite Structures*, Vol. 244, pp. 112320, 2020.
- [76] R. Selvamani, M. M. S. Jayan, R. Dimitri, F. Tornabene, F. Ebrahimi, Nonlinear magneto-thermo-elastic vibration of mass sensor armchair carbon nanotube resting on an elastic substrate, *Curved and Layered Structures*, Vol. 7, No. 1, pp. 153-165, 2020.

- [77] S. Asghar, M. N. Naeem, M. Hussain, M. Taj, A. Tounsi, Prediction and assessment of nonlocal natural frequencies of DWCNTs: Vibration analysis, *Computers and Concrete, An International Journal*, Vol. 25, No. 2, pp. 133-144, 2020.
- [78] H. Dai, H. Safarpour, Frequency and thermal buckling information of laminated composite doubly curved open nanoshell, *Advances in nano research*, Vol. 10, No. 1, pp. 1-14, 2021.
- [79] W. Weng, Y. Lu, V. Borjalilou, Size-dependent thermoelastic vibrations of Timoshenko nanobeams by taking into account dual-phase-lagging effect, *The European Physical Journal Plus*, Vol. 136, pp. 1-26, 2021.
- [80] X. Yue, X. Yue, V. Borjalilou, Generalized thermoelasticity model of nonlocal strain gradient Timoshenko nanobeams, *Archives of Civil and Mechanical Engineering*, Vol. 21, No. 3, pp. 124, 2021.
- [81] H. Danesh, M. Javanbakht, Free vibration analysis of nonlocal nanobeams: a comparison of the one-dimensional nonlocal integral Timoshenko beam theory with the two-dimensional nonlocal integral elasticity theory, *Mathematics and Mechanics of Solids*, Vol. 27, No. 4, pp. 557-577, 2022.
- [82] M. Fakher, S. Hosseini-Hashemi, Vibration of two-phase local/nonlocal Timoshenko nanobeams with an efficient shear-locking-free finite-element model and exact solution, *Engineering with Computers*, pp. 1-15, 2022.
- [83] M. Espo, S. M. Hosseini, M. H. Abolbashari, Bandgap characteristics of a piezoelectric phononic crystal Timoshenko nanobeam based on the modified couple stress and surface energy theories, *Materials Today Communications*, Vol. 33, pp. 104782, 2022.
- [84] M. Eltaher, R. Shanab, N. Mohamed, Analytical solution of free vibration of viscoelastic perforated nanobeam, *Archive of Applied Mechanics*, Vol. 93, No. 1, pp. 221-243, 2023.
- [85] Ö. Civalek, B. Uzun, M. Ö. Yaylı, Thermal buckling analysis of a saturated porous thick nanobeam with arbitrary boundary conditions, *Journal of Thermal Stresses*, Vol. 46, No. 1, pp. 1-21, 2023.
- [86] A. Eyvazian, C. Zhang, M. Alkhdher, S. Muhsen, M. A. Elkotb, Thermal buckling and post-buckling analyses of rotating Timoshenko microbeams reinforced with graphene platelet, *Composite Structures*, Vol. 304, pp. 116358, 2023.
- [87] K. Boyina, R. Piska, Wave propagation analysis in viscoelastic Timoshenko nanobeams under surface and magnetic field effects based on nonlocal strain gradient theory, *Applied Mathematics and Computation*, Vol. 439, pp. 127580, 2023.
- [88] M. Soltani, B. Asgarian, Finite element formulation for linear stability analysis of axially functionally graded nonprismatic timoshenko beam, *International Journal of Structural Stability and dynamics*, Vol. 19, No. 02, pp. 1950002, 2019.
- [89] M. Soltani, B. Asgarian, F. Jafarzadeh, Finite difference method for buckling analysis of tapered Timoshenko beam made of functionally graded material, *AUT Journal of Civil Engineering*, Vol. 4, No. 1, pp. 91-102, 2020.
- [90] M. Soltani, A. Gholamizadeh, Size-dependent buckling analysis of non-prismatic Timoshenko nanobeams made of FGMs rested on Winkler foundation, *Journal of Numerical Methods in Civil Engineering*, Vol. 3, No. 2, pp. 35-46, 2018.
- [91] R. Bellman, J. Casti, Differential quadrature and long-term integration, *Journal of mathematical analysis and Applications*, Vol. 34, No. 2, pp. 235-238, 1971.
- [92] A. Soltani, M. Soltani, Comparative study on the lateral stability strength of laminated composite and fiber-metal laminated I-shaped cross-section beams, *Journal of Computational Applied Mechanics*, Vol. 53, No. 2, pp. 190-203, 2022.
- [93] C. W. Bert, M. Malik, Differential quadrature method in computational mechanics: a review, 1996.
- [94] M. Soltani, Finite element modeling for buckling analysis of tapered axially functionally graded timoshenko beam on elastic foundation, *Mechanics of Advanced Composite Structures*, Vol. 7, No. 2, pp. 203-218, 2020.
- [95] M. Soltani, A. Soltani, O. Civalek, Interaction of the lateral buckling strength with the axial load for FG micro-sized I-section beam-columns, *Thin-Walled Structures*, Vol. 179, pp. 109616, 2022.
- [96] A. Shahba, R. Attarnejad, M. T. Marvi, S. Hajilar, Free vibration and stability analysis of axially functionally graded tapered Timoshenko beams with classical and non-classical boundary conditions, *Composites Part B: Engineering*, Vol. 42, No. 4, pp. 801-808, 2011.